

Damage Detection and Identification in Structures by Spatial Wavelet Based Approach

D. Mallikarjuna Reddy^{a,*} and S. Swarnamani^b

^a*Mechanical Engineer, Chennai-73, India*

^b*Mechanical Engineering Department, Indian Institute of Technology Madras, Chennai-36, India*

Abstract: The objective of current work is to show the effectiveness of using wavelet transform for detection and localization of small damages. The spatial data used here are the mode shapes and strain energy data of the damaged plate. Because the wavelet coefficients are performed with various scale indices, local perturbations in the mode shapes and strain energy data can be found in the finer scale that are positioned at the locations of the perturbations. The continuous wavelet transform (CWT) using complex Gaussian wavelet with four vanishing moments is used to get the spatially distributed wavelet coefficients so as to identify the damage position on a square plate. The mode shape and strain energy data of the square plate with damage of different sizes are obtained by using ANSYS 9.0. The damage is simulated by reducing the thickness of one element out of 625 elements used for modeling. It is observed that by using modal data as input, damage can be identified if the reduction in thickness in one of the elements is at least 10%. Use of strain energy data as input to the wavelet analysis provides detection up to less than 10% damage. Lipschitz (Hoelder) exponent (α) and Intensity factor (K) is derived from the coefficients to quantify the relation between damage and change in wavelet coefficients derived from modal and elemental strain energy data. The variation of maximum absolute wavelet coefficients versus percentage of damage for different mode shapes and scales are studied Influence of boundary conditions of the plate on damage identification has been studied, especially for damage near boundaries. Another objective of this paper is to apply wavelet transform to highlight the detection and localization of damage in beam and stiffened panel using experimental modal data as input to the wavelet analysis. This in real time has potential to be used in structural damage monitoring.

Keywords: Structural health monitoring; damage detection; modal analysis; spatial wavelets; lipschitz (hoelder) exponent.

1. Introduction

Damage in a mechanical (or) structural system may be contributed by various factors, such as excessive response, accumulative crack growth, wear and tear of working parts, and impact by a foreign object. Structural Health Monitoring (SHM) has emerged as a

reliable, efficient and economical approach to monitor the system performance, detect such damage, asses/diagnose the structural health condition, and make corresponding maintenance decisions; consequently, structural safety and functionality will be significantly

* Corresponding author; e-mail: dmreddy_iitm@rediffmail.com
© 2012 Chaoyang University of Technology, ISSN 1727-2394

Received 1 September 2011
Revised 14 October 2011
Accepted 13 January 2012

improved and a condition based maintenance procedure can be developed. Due to localization of damage in structures techniques using global averaging procedures, applied to changes in eigen frequencies are less sensitive to initial or small changes. Hence recent techniques that process the local changes in the structural parameters based on wavelets have emerged recently. An application of spatial wavelet theory to damage identification in structures was proposed by Liew and Wang [1]. They calculated the wavelet coefficients along the length of the beam based on the numerical solution for the deflection of the beam, the damage location was then indicated by a peak in the coefficients of the wavelets along the length of the beam. Wang and Deng [2] described a method for detecting the location of localized defects. Quek, Wang, Zhang and Ang, [3] also used wavelet analysis for crack identification in beams under both simply supported and fixed–fixed boundary conditions. Abdo and Hori [4] made numerical study of the relation between damage characteristics and changes in the dynamic properties. It is found the rotation mode shape has the characteristic of localization at the damaged region even though the displacement modes do not localize damage. Hong, Kim and Lee [5] used the Lipschitz exponent for the detection of singularities in beam modal data. The Mexican hat wavelet was used and the damage extent was related to different values of the exponent. The correlation, however, of the extent of damage to the Lipschitz exponent is sensitive to both sampling distance and noise resulting in limited accuracy of prediction. Recently, an interesting comparison between a frequency-based and mode shape-based method for damage identification in beam like structure has been published by Kim, Ryu, Cho, and Stubbs [6]. Douka, Loutridis and Trochidis [7] presented a method for crack identification in plate structures based on wavelet analysis is presented. The vibration modes of plate having a crack parallel to the one edge are wavelet transformed and

both the location and depth of the crack are estimated. Later Chang and Chen [8] used Gabor wavelet transform for spatially distributed modes so that the distributions of wavelet coefficients could identify the damage position on a rectangular plate by showing a peak at the position of the damage. Chang and Chen [9] also presented both the positions and depths of multi-cracks can be estimated from spatial wavelet based method. Rucka and Wilde [10] demonstrated estimating the damage location in beam and plate structure using wavelet analysis using both experimental and analytical mode shape data.

Despite the extensive studies of vibration analysis on damaged plates, only few effective and practical techniques are found for very small damaged identification. This paper, therefore, focuses on study of a practical method using Lipschitz (Hoelder) exponent on spatial wavelet data for effective identification of damages in plate structure by combining numerical modal analysis (using ANSYS) with continuous wavelet transform. The sensitivities of two spatial inputs namely displacement mode shape and strain energy data to damage identification are found to be markedly improved. Influence of boundary conditions of the plate on damage identification has been studied, especially for damage near boundaries. Also shown the crack identification in plate structure for different modes

2. Formulation

2.1. Numerical Simulation

The dimension of plate under consideration is 0.25m x 0.25m x 0.003 m with Fixed – Fixed support condition as shown in Figure 1. The material properties used in modeling the plate is listed in Table 1. E (68.9 GPa), ν (0.33) and ρ (2710 Kg/m³) refer to Young Modulus, Poisson ratio and Mass Density respectively. The Element type selected for modeling plate is Shell Elastic 4 node 63 which has six degrees of freedom in ANSYS 9.0.

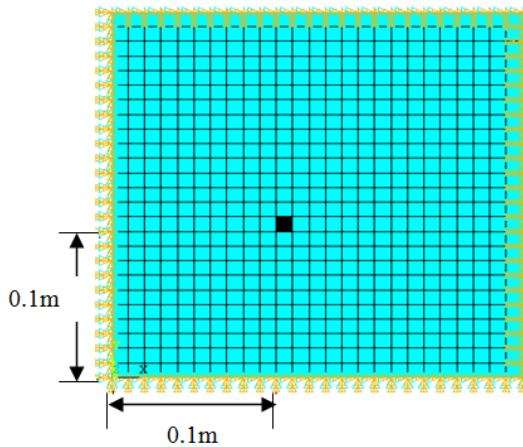


Figure 1. Damaged plate model from ANSYS 9.0 with element reduced thickness.

The Length and width of plate is equally divided into 25 elements so the simulated model has total of 625 elements. Damage is simulated by reducing the thickness of one element at location shown (0.1, 0.1m) shown in Figure 1. The mode shape and elemental strain energy data of the square plate with damage of different sizes are obtained

2.2. Fundamentals of wavelet analysis

As an extension of traditional Fourier transform, the advantage of wavelet analysis lies in its characteristics to provide the time and frequency information simultaneously. The wavelet analysis for such application was proposed by Grossman and Morlet [11]. However, due to its mathematical complexity, the study of wavelet theory was not fully explored. It is the work done by Mallat [12], Daubechies [13] that built up the relationship between the theory and the application of wavelet analysis.

Wavelets are usually used to analyze signals in the time domain. However, by replacing time variable t with a spatial coordinates, spatially distributed mode shapes can be also analyzed. For square-integrable one dimensional signal $f(x)$, the Continuous Wavelet Transform Wf is defined as

$$Wf(u, s) = \int_{-\infty}^{+\infty} f(x) \psi_{u,s}^*(x) dx = \int_{-\infty}^{+\infty} f(x) \frac{1}{\sqrt{s}} \psi^* \left(\frac{x-u}{s} \right) dx \quad (1)$$

Where $\psi^*(x)$ is the conjugate of the mother wavelet $\psi(x)$. The function $\psi_{u,s}(x)$ is dilated by the scaling parameter 's' and translated by the translation parameter 'u' of the mother wavelet $\psi(x)$. Considering a two dimensional spatial signals to distribute over $[0, Lx]$ in the x direction and $[0, Ly]$ in the y direction, the wavelet coefficients for the signal then can be written as [6]

$$W_{\psi} = \int_0^{Ly} \left(\int_0^{Lx} s(x, y) \psi_{u,s}^*(x) dx \right) \psi_{u,s}^*(y) dy \quad (2)$$

So for the wavelet analysis in the x direction we have

$$W_{\psi}(u, s, y) = \int_0^{Lx} s(x, y) \psi_{u,s}^*(x) dx \quad (3)$$

Similarly in y direction we have

$$W_{\psi}(u, s, x) = \int_0^{Ly} s(x, y) \psi_{u,s}^*(y) dy \quad (4)$$

The family of wavelets used, the Complex Gaussian wavelets, generated from the complex Gaussian function. It is defined as derivatives of the complex Gaussian function.

$$cgau(x) = c_n * \text{diff}(\exp(-i * x) * \exp(-x^2), n) \quad (5)$$

Where 'diff' denotes the symbolic derivative and where C_n is a constant.

The procedure of the damage detection is as follows:

- (1) Find the analytical mode shapes of the structure.
- (2) Calculate the spatial wavelet coefficients of the mode shapes.
- (3) Plot the value of wavelet coefficients in the full region for each scale of wavelets.
- (4) Examine the distributions of wavelet coefficients at each scale. A sudden change in the distributions of the wavelet coefficients identifies the damage position.

2.3. Lipschitz (Hoelder) exponent and Intensity factor

An important property of the CWT is the ability to characterize the local regularity of functions. The Hoelder exponent α often measures this local regularity. A function $f(x)$ is said to be Hoelder $\alpha \geq 0$ at $x=v$ if there exists constant $K>0$ and a polynomial p_v of degree m (where m is the largest integer satisfying $m \leq \alpha$) such that [14]

$$|f(x) - p_v(x)| \leq K |x - v|^\alpha \tag{6}$$

By examining the decay of wavelet maxima coefficients as scale s tends to zero it is proved [9] that, for isolated singularities, the wavelet maxima obeys an exponential law with an exponent equal to Hoelder exponent α , given by

$$|Wf(u, s)| \leq K s^{\alpha+(1/2)} \tag{7}$$

In order to estimate α numerically, rewriting Eq (7) in logarithmic form gives

$$\log_2 |Wf(u, s)| \leq \log_2 K + \left(\alpha + \frac{1}{2} \right) \log_2 s \tag{8}$$

The Hoelder exponent and Intensity factor K are estimated by linear interpolation so that the squared error is minimized. The Hoelder exponent gives information about differentiability of a function more precisely. The value of Hoelder exponent at a point depends on, the more regular is the function at that point. By knowing the slope α and Intensity factor K the size of damage can be estimated.

3. Results and discussions

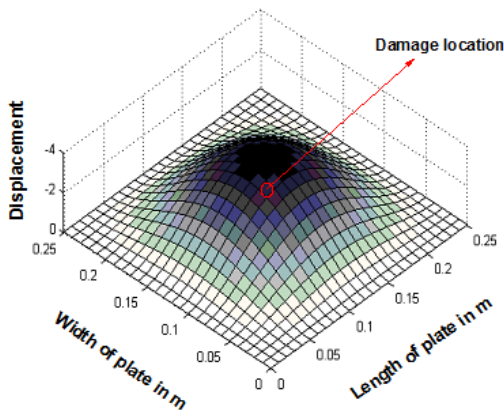
The mode shapes and strain energy data of the damaged plate with the region of reduced stiffness are analyzed by the wavelet transform to see if local perturbations can be observed at the damage position. Table.1 gives the natural frequencies of first three modes before and after damage.

Table 1. Comparison of natural frequencies (Hz) for undamaged and damaged cases

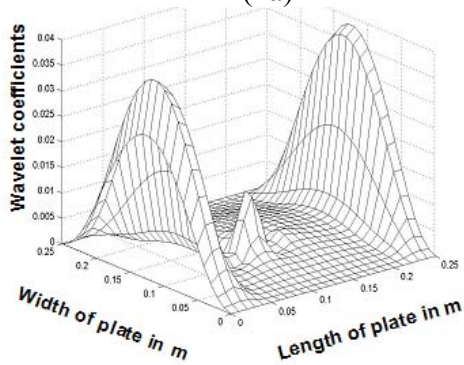
Panel details	Frequencies (Hz) of mode shapes		
	1	2	3
Undamaged	423.41	863.09	863.12
Damaged	423.30	861.79	862.76

The variations in frequencies shown are quite small and hence processing of mode shape data using wavelet transform has been attempted. The first mode shape of the damaged plate with thickness reduced from 0.003m to 0.002m is shown in Figure 2 located at 0.1m in x direction and 0.1m in y direction. It is observed the mode shape data of Figure.2a does not indicate damage position. Figures 2b show plot of wavelet coefficients in x direction at scale $s = 2$ giving clear indication of a peak at point of damage location. Figure 2c shows the variation of two dimensional wavelet coefficients plot that include the damaged region along the length of the plate. In order to detect the damage position, the mode shape is wavelet transformed using complex Gaussian wavelet with four vanishing moments. High value of s corresponds to broad wavelets, so that low frequencies can be looked through, while a low value of s corresponds to narrow wavelet suitable for the analysis of high frequency components. Since Damages corresponds to high frequency components scales, wavelet scales of 1, 2 and 3 are used in present analysis.

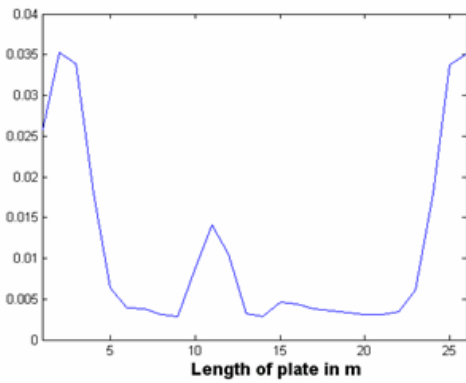
It is shown that the values of wavelet coefficients at the damaged region shows distinct changes in slope compared to other undamaged region. The reason is that there is the geometric discontinuity at that position so the changes of deflection are larger at that region and local perturbations can also be detected by wavelet analysis.



(2a)

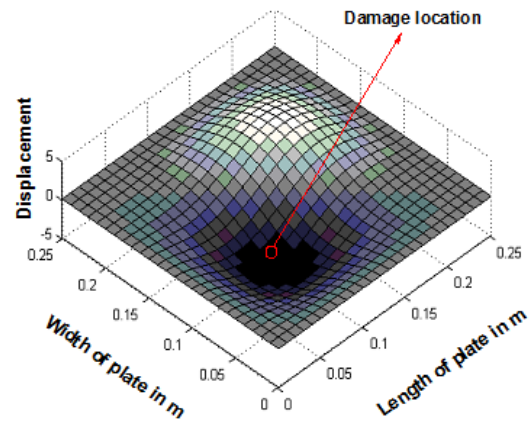


(2b)

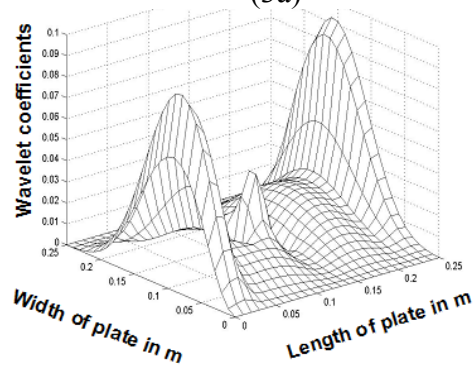


(2c)

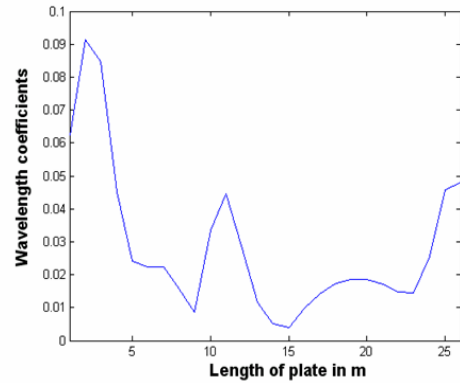
Figure 2. (a) The first mode shape of the (33.33%) damaged plate. (The boundary conditions are clamped at four edges), (b) The distributions of wavelet coefficients in x direction for scale parameter ($s = 2$) respectively based on the first mode shape, (c) Two dimensional wavelet coefficients plot ($s = 2$, x direction) along the length of the plate including the damaged element



(3a)

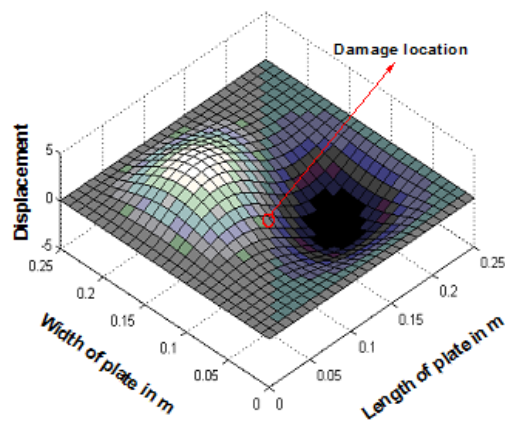


(3b)

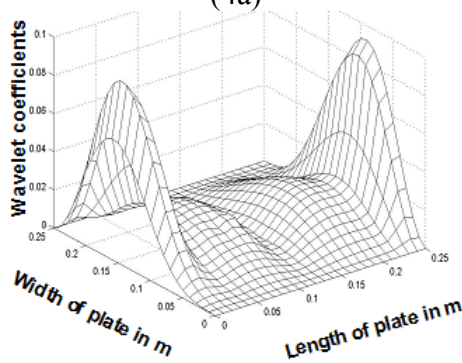


(3c)

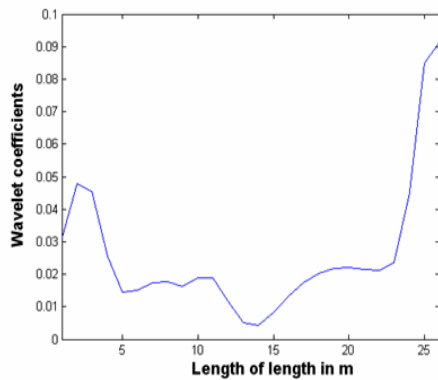
Figure 3. (a) The second mode shape of the (33.33%) damaged plate. (The boundary conditions are clamped at four edges), (b) The distributions of wavelet coefficients in x direction for scale parameter ($s = 2$) respectively based on the second mode shape, (c) Two dimensional wavelet coefficients plot ($s = 2$, x direction) along the length of the plate including the damaged element



(4a)



(4b)



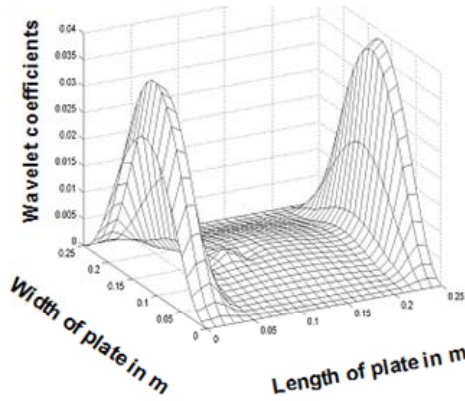
(4c)

Figure 4. (a) The third mode shape of the (33.33%) damaged plate. (The boundary conditions are clamped at four edges), (b) The distributions of wavelet coefficients in x direction for scale parameter ($s = 2$) respectively based on the third mode shape, (c) Two dimensional Wavelet coefficients plot ($s = 2$, x direction) along the length of the plate including the damaged element

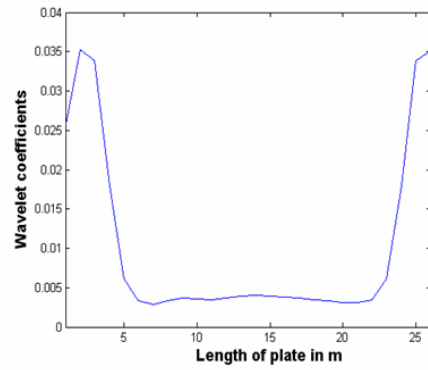
Similar set of data for the second and third mode shapes are presented in Figure (3a – 3c), (4a – 4c) respectively. It is also observed that wavelet analysis can be used to detect the damage position. The modal amplitude at the damage location is highest for second mode (Figure 3a) and lowest for third mode (Figure 4a) because the damage location lies at the antinodes location in second mode where as in third mode lies on nodal line i.e. nodal point where there is no displacement. Therefore the maximum wavelet coefficients plotted using the second mode shows higher value at damaged location Figure 3c compare to first and third mode.

Since the damaged location at the mode of the third mode the value of maximum wavelet coefficients is marginal. It is observed that by using modal data as input, damage can be identified reasonably well if the reduction in thickness is not less than 10% (equivalent stiffness reduction by 27.1%). Figure 5a shows wavelet distributions plot at scale 2 for 10% damage and Figure 5b show the corresponding two dimensional wavelet plot along the length of the plate at damaged element. It is observed that there is no clear distinct change in slope at damaged region for 10% damage.

Figure 6a shows wavelet distribution plot given elemental strain energy as input for the 10% damage case for same scale. The corresponding wavelet coefficient plot clearly indicates increase in slope at damaged site as shown in Figure 6b. It is observed that the method using strain energy data is much more sensitive to damage than the method which uses mode shape as input to the wavelet.

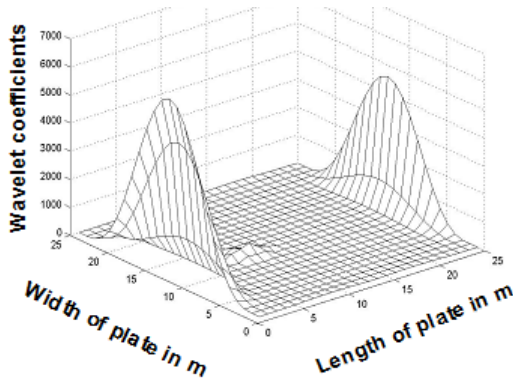


(5a)

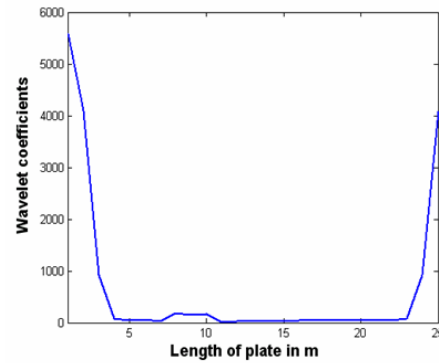


(5b)

Figure 5. (a) The distributions of wavelet coefficients in x direction only for first mode shape for 10% damage case with scale parameter ($s = 2$) based on the first mode shape, (b) Two dimensional Wavelet coefficients plot ($s = 2$) along the length of the plate at damaged element



(6a)



(6b)

Figure 6. (a) Elemental Strain Energy data first mode based wavelet coefficients plot with damaged location, (b) The trend of two dimensional wavelet coefficients plot ($s = 2$) at damage location long the length of plate

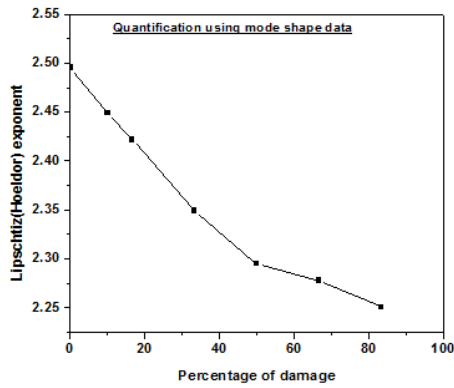
3.2. Damage quantification

To investigate the relation between percentage of damage extent and lipschitz exponent, plot of estimated lipschitz exponent as function of percentage of damage values is shown in Figure 7. Figure 7a, and 7b shows plot of estimated lipschitz exponent for mode shape data and elemental strain energy data respectively to quantify damage severity.

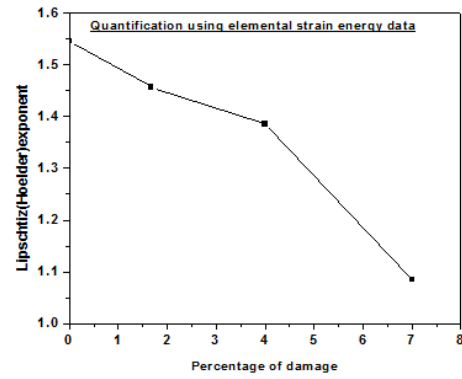
It is evident from plots that as damage severity increases the lipschitz exponent ' α ' decreases .which indicates that the smoothness of curve decreases at the damaged loca-

tion. Similar way In order to quantify the relation between percentage of damage and change in wavelet coefficients derived from modal data, a factor called Intensity factor is derived from the coefficients is shown in Figure 8.

The intensity of factor is the inverse of Hoelder (Lipschitz) exponent which varies with increase in damage. Figure 8a, and 8b shows plot of estimated Intensity of factor for mode shape data and elemental strain energy data respectively to quantify damage severity. It is evident from plot that as damage severity increases the Intensity of factor 'K' decreases.

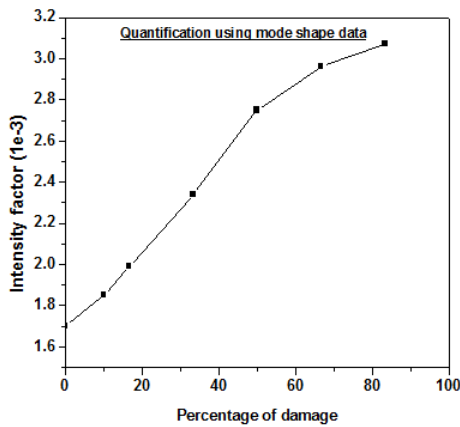


(7a)

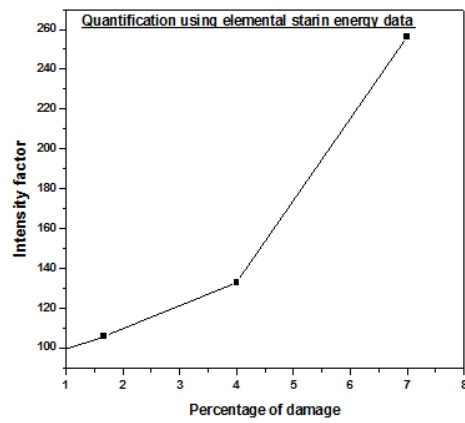


(7b)

Figure 7. Variation of Lipschitz (Hoelder) exponent (α) at damage site for different damage cases (a) using mode shape data, (b) using elemental strain energy data



(8a)



(8b)

Figure 8. Variation of Intensity factor K at damage site for different damage cases (a) using mode shape data, (b) using elemental strain energy data

For the quantification of damage and also to ascertain the sensitivity of particular mode used, the variation of maximum absolute wavelet coefficients versus percentage of damage for different mode shapes and scales is plotted as shown in Figure 9. It is observed that the absolute wavelet coefficients increase with increase in damage severity. For some modes by comparing the sensitivity of different modes it is found that the first mode at scale 1, 2 is much more sensitive to damage for the chosen damage location than other modes and scales.

3.3 Multiple damage identification

The proposed method can clearly locate the multiple damage locations on the plate structures. Figures 10a show plot of wavelet coefficients in x direction at scale $s = 2$ for first mode shape giving clear indication of a peaks at point of damage locations.

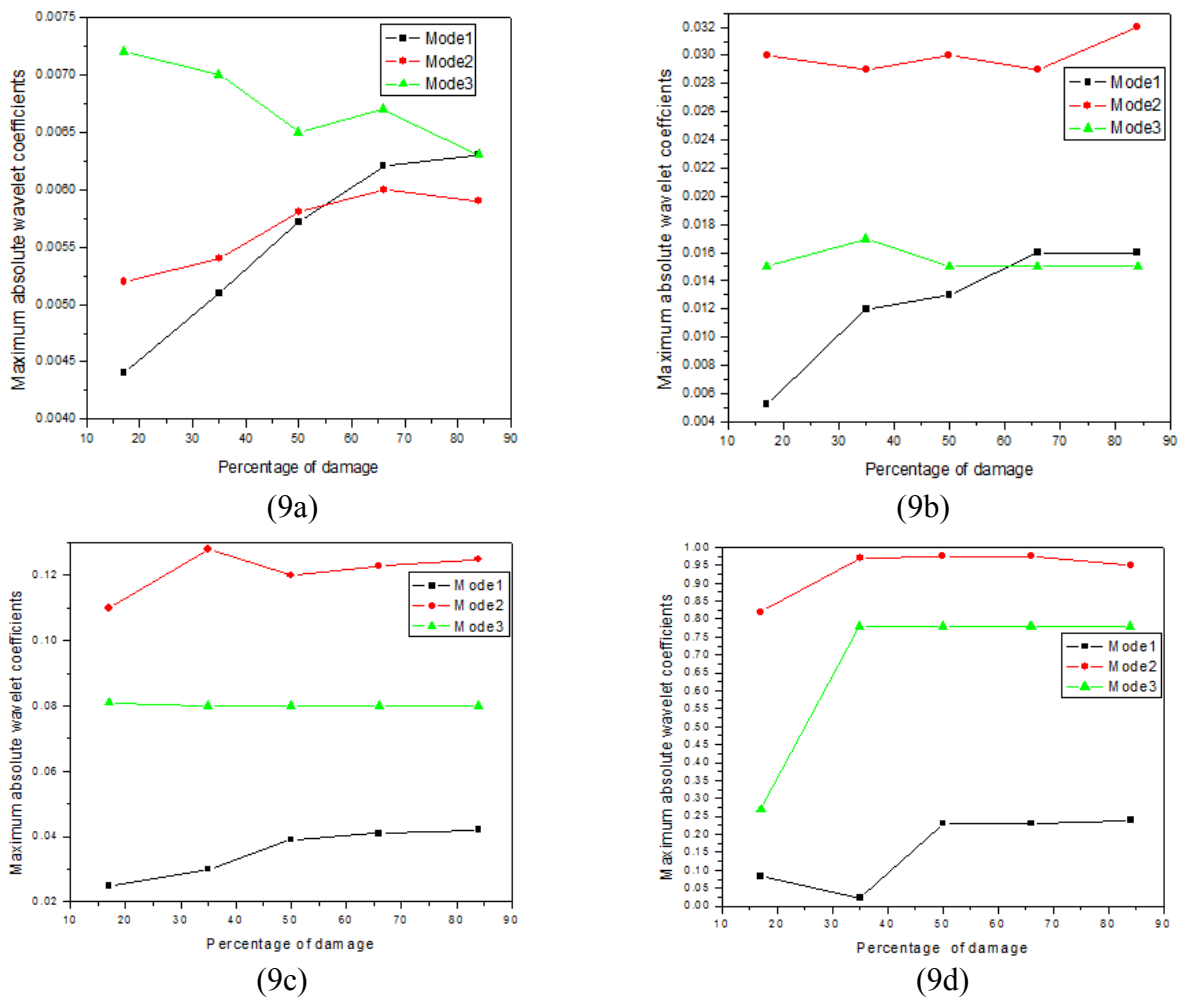


Figure 9. Variation of maximum absolute wavelet coefficients versus percentage of damage for mode 1, 2 and 3 at scale (a) 1, (b) 2, (c) 3, (d) 5

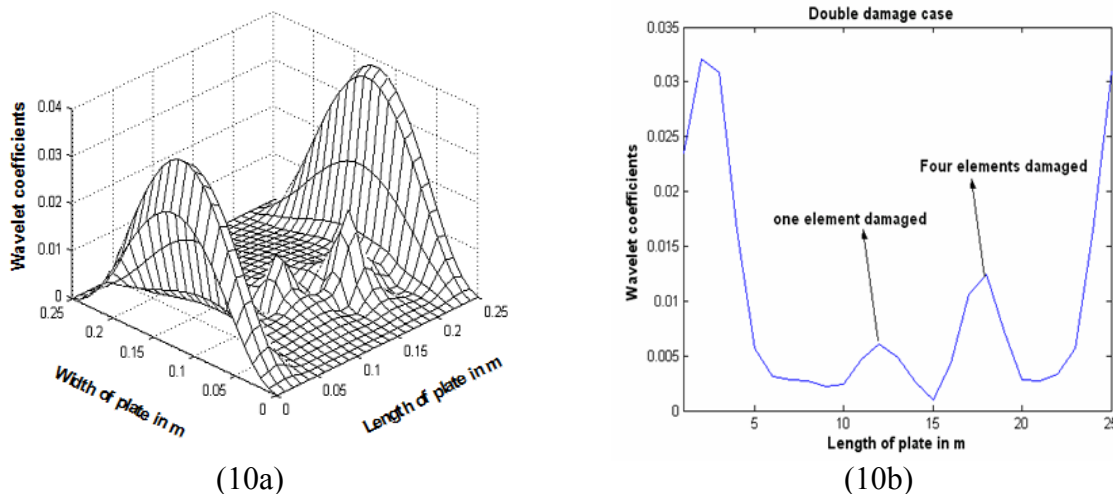


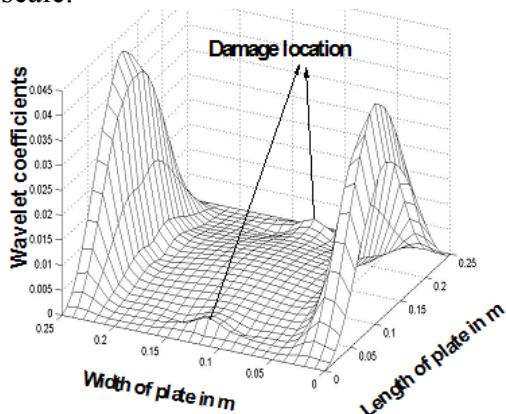
Figure 10. (a) The distributions of wavelet coefficients in x direction only for first mode shape for 33.33% (Reduction in stiffness 96.2%) damage case with scale parameter ($s = 2$) based on the first mode shape, (b) Two dimensional Wavelet coefficients plot ($s = 2$) along the length of the plate at damaged elements

Figure 10b shows the variation of two dimensional wavelet coefficients plot that include the damaged region along the length of the plate. From this analysis easily identify the small and large damages by comparing the variation of wavelet coefficients.

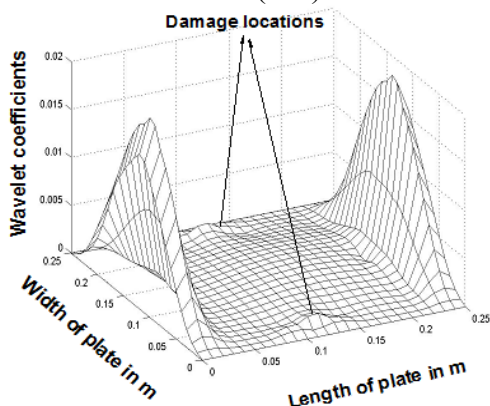
4. Influence of boundary conditions on damage identification

4.1. Using displacement mode shape and strain energy data

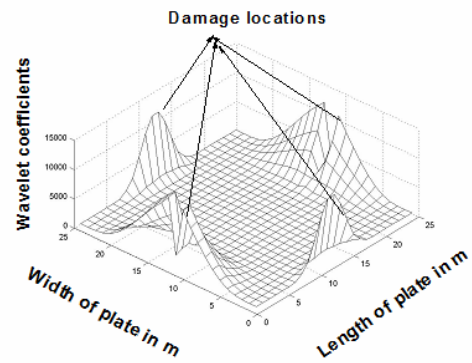
Effectiveness of using a three dimensional plot of wavelet coefficients is strongly dependent on type of boundary conditions. As certain boundary conditions of plate can cause coefficients to be extremely high at the boundaries plotting coefficients on the whole domain of the plate may cause the true damage invisible when plotted in the relative scale.



(11a)



(11b)



(11c)

Figure 11. (a) and (b) 3-D Wavelet plots where coefficients plotted in x and y directions respectively on whole domain of plate (Fixed -Fixed boundary) for damage at four locations along four edges, (c) Elemental strain energy data first mode based wavelet coefficients plot ($s = 2$) with damaged location at boundaries

4.1.1. Fixed - fixed condition

This depends upon convolution operated by CWT which assumes the input spatial signal spread over infinite space. Because of input data having finite interval as in the present case with mode shape, the CWT gives higher value of coefficients at the boundary due to presence of discontinuing slope. In Figure 11a, 11b show the wavelet coefficients plotted along x and y directions at scale $s = 2$ respectively for first mode shape and elemental strain energy data for damage near the clamped edges of plate respectively with clear indication of peak at point of damage location. Plotting wavelet coefficients in both x and y directions are necessary to find out damages near boundaries. It is seen that the wavelet coefficients at the boundaries are less that it is possible to locate damage.

4.1.2. Free - Free boundary condition

Similar analysis has been repeated for the same plate with free-free condition. The damage is simulated by reducing the thickness of two elements at centre of the all four

edges of plate. Processing of mode shape data and strain energy data using wavelet transform has been attempted. Figure 12a shows the first bending mode shape of plate. Figure 12b shows corresponding plot of three dimensional

wavelet coefficients. Figure 12c show the wavelet coefficients plot at scale $s = 2$ for mode shape in logarithmic scale so as to improve damage detection.

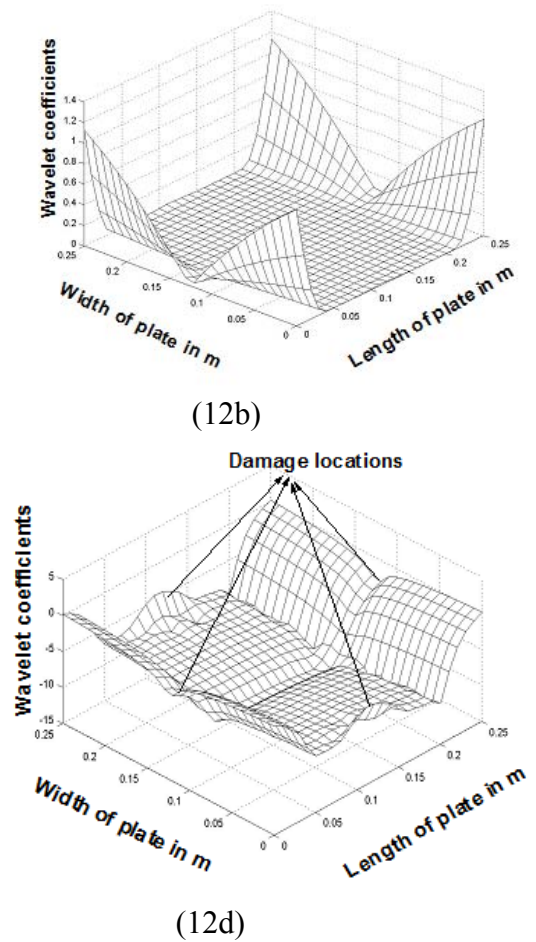
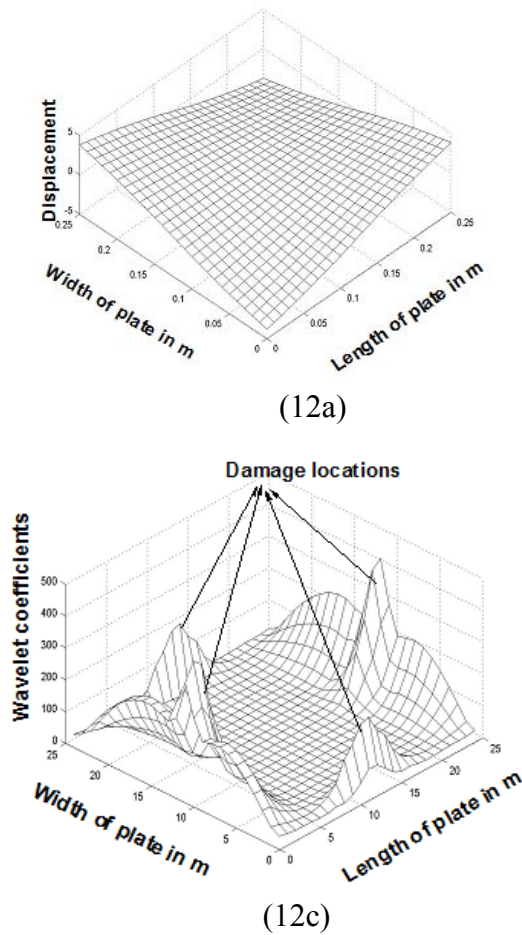


Figure 12. (a) The first bending mode shape of the damaged plate. (The boundary conditions are free at four edges), (b) The distributions of wavelet coefficients for scale parameter ($s = 2$) based on the corresponding mode shape, (c) The distributions of wavelet coefficients in logarithmic scale for scale parameter ($s = 2$), (d) Elemental strain energy data first mode based wavelet coefficients plot ($s = 2$) with damaged location at boundaries

Figure 12d shows plot of elemental strain energy data with clear indication of peak at point of damage location. It is seen that the coefficients at the free boundaries are so high that it is impossible to identify influence of damage. To improve visibility of damage to some extent, plotting the wavelet coefficients in logarithmic scale seems to help as shown in Figure 12c, which distinctly indicate the

damage area even when there are high coefficients values in the neighborhood at the free boundaries. Figure 12d shows wavelet coefficients of elemental strain energy data, without logarithmic plot, with clear indication of peaks showing at damage at boundaries.

The damage is simulated by reducing the thickness of two elements at centre of the all four edges of plate. Processing of mode shape

data and strain energy data using wavelet transform has been attempted. Figure 12a shows the first bending mode shape of plate. Figure 12b shows corresponding plot of three dimensional wavelet coefficients. Figure 12c show the wavelet coefficients plot at scale $s = 2$ for mode shape in logarithmic scale so as to improve damage detection. Figure 12d shows plot of elemental strain energy data with clear indication of peak at point of damage location.

It is seen that the coefficients at the free boundaries are so high that it is impossible to identify influence of damage. To improve visibility of damage to some extent, plotting the wavelet coefficients in logarithmic scale seems to help as shown in Figure 12c, which distinctly indicate the damage area even when there are high coefficients values in the neighborhood at the free boundaries. Figure 12d shows wavelet coefficients of elemental strain energy data, without logarithmic plot, with clear indication of pecks showing at damage at boundaries.

5. Experimental verification

In order to test the feasibility of applying proposed wavelet based damage identification method to experimental data (mode shape), experimental modal analysis is carried out on a simple steel beam with free-free boundary condition. This is particularly necessary because the experimentally obtained mode shape is distorted with noise. Hence the effectiveness of the method with noisy mode shape as input can be investigated.

5.1. Experimental modal analysis

For experimentation, a steel beam with rectangular cross section of dimension 700 x 30 mm is considered. The schematic diagram showing the experimental setup is

shown in Figure 13. The beam is supported by a thin nylon rope with flexible springs to simulate free-free boundary conditions. In order to acquire fundamental mode shape accurately the beam is supported at the nodal points of first mode shape.

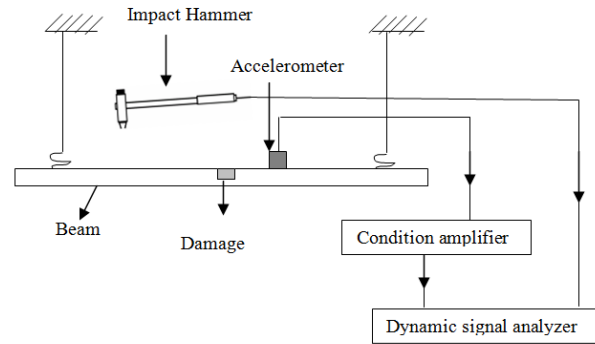
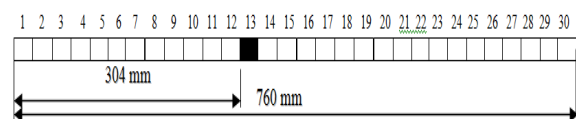


Figure 13. Schematic diagram of experimental set up

A miniature accelerometer used to measure the response is firmly fixed near the middle of the beam with a bee wax. The beam is excited by using impact hammer and the resulting data has been acquired by Dynamic Signal Analyzer. The acquired signal has been averaged twice in frequency domain. Acquired frequency response functions at different locations from Dynamic Signal Analyzer are given as input to modal analysis software (LMS CADA PC MODAL) to get natural frequencies and mode shape. The vibration data is acquired at 31 discrete points with a spatial distance of 25.4 mm as shown in Figure 14. The damage is artificially introduced by a symmetric wide slot in 13th element (at 304 mm from left end) of the beam as shown in Figure (14b), the width (w) of which is 25.4 mm. Experimental mode shapes are measured for three different cases of damage with damage $c/h = 0.1, 0.15$ and 0.2 .



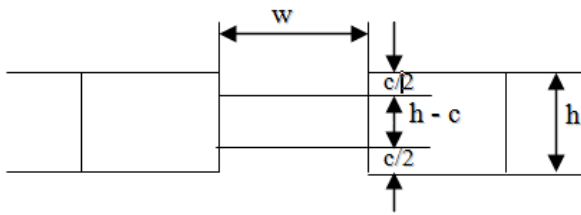


Figure 14. Beam dimension and damage geometry used in experiment

5.2. Results and Discussions

First the undamaged beam is considered and the natural frequencies is compared to the numerically results obtained by using the same dimension, material property and boundary condition. Table 2 shows the first four natural frequencies for undamaged beam which shows that there slight acceptable difference between the numerical and experimental results.

Table 2. First four natural frequencies of undamaged beam

Mode No	Natural frequencies	
	FEM(MATLAB)	Ex-perimental
1	180.88	181.70
2	498.61	498.48
3	977.49	970.02
4	1615.9	1592.0

Table 3. Comparison of experimentally obtained first four natural frequencies for undamaged and damaged beam

Mode No	Experimental results	
	Undamaged	c/h=0.1
1	181.70	179.079
2	498.89	496.201
3	970.02	968.010
4	1592.0	1579.0

Table 3 shows the first four natural frequencies for beam with damage c/h of 0.1 obtained as output from LMS CADA modal analysis software. The fundamental mode shape as shown in Figure 15 has 31 spatial sampling points one at each discrete points. Because of sparse sampling, the wavelet transform if implemented directly would detect many points of sampled data as singularities. Therefore, to smooth the transition from one point to another an, a cubic spline interpolation has been used to obtain 301 equally spaced points along the length. This mode shape with increased spatial sampling points is wavelet transformed and the 3-D plot of wavelet coefficients is shown in Figure 16(b).

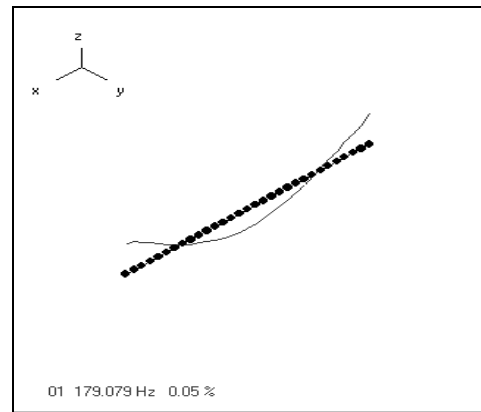
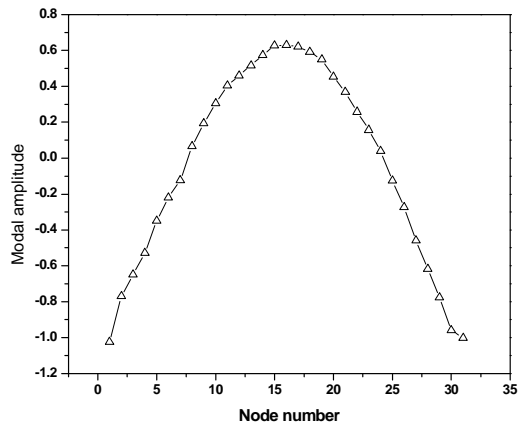
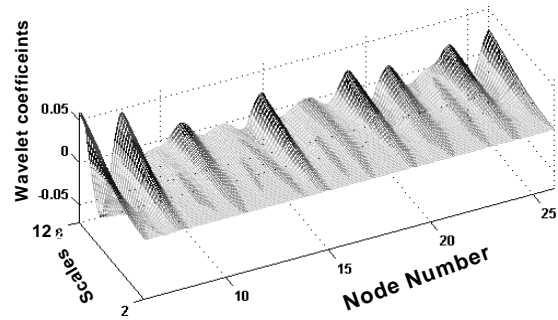


Figure 15. First fundamental mode shape obtained from LMS CADA modal analysis software

It is found from Figure 16(b) that, there are high wavelet coefficients at the damaged element (13th element) indicating damage. But there are many points of high wavelet coefficients all along the length giving false indication of damages. This indicates that the measured mode shape signal does not contain the perturbation in curvature caused due to damage, because of which wavelet transform method failed to detect damage correctly.

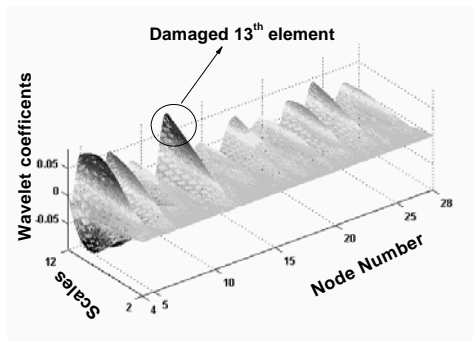


(16a)

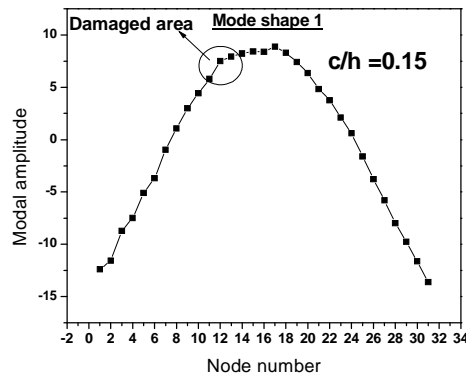


(16b)

Figure 16. Damage identification with damage $c/h=0.1$ at 13th element (a) Fundamental mode shape from damaged beam ($c/h=0.1$), (b) 3-D wavelet plot

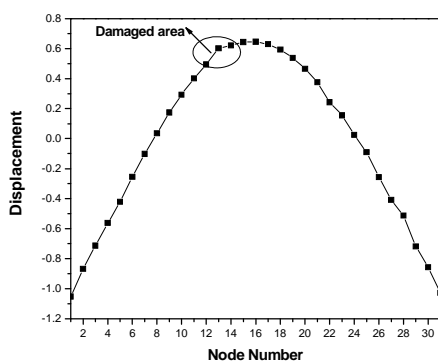


(17a)

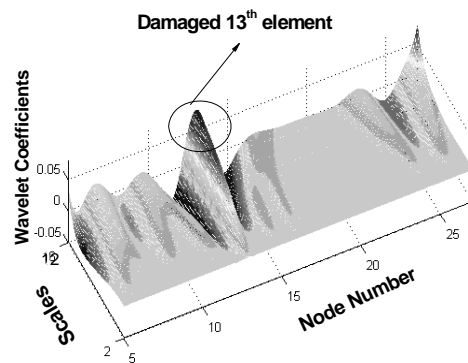


(17b)

Figure 17. Damage case $c/h=0.15$ (a) Experimental mode shape, (b) 3-D Wavelet plot



(18a)



(18b)

Figure 18. Damage case $c/h=0.2$ (a) Experimental mode shape, (b) 3-D Wavelet plot

Figure 17(a) shows the experimentally obtained fundamental mode shape for c/h of

0.15 and corresponding wavelet plot is shown in Figure 17 (b). Even though there are many

points of high wavelet coefficients other than damaged point, there is high relatively coefficients at the damage element as indicated in Figure 17 (b).

Figure 18 shows similar plots for higher damage ($c/h=0.2$). It is observed from the Figure 18 (b) that is single points at which there is relatively large wavelet coefficients at the damage location.

It is found that the method is able to correctly locate damage in case of c/h of 0.2 and 0.15 for damage at single element number 13. This method failed to identify damage in case of $c/h=0.1$ because the mode shape measured did not contain information of damage in terms of changes in curvature at the damage location. Hence this wavelet based damage identification method strongly depends on the measurement methods used to acquire spatial data, the accuracy and the measurement noise. This method is particularly suitable, when the vibration data is obtained from laser vibrometer or optic fiber sensor (non-contact type) which provides data with high accuracy and high spatial density.

6. Experimental based damage localization in a stiffened panel using wavelet approach

In this paper a novel method for damage identification in stiffened panel based on wavelet analysis is presented. This method only needs the spatially distributed displacements or mode shapes. First the natural frequencies and mode shapes of healthy and damaged panel are obtained experimentally. Then, the mode shape that is very sensitive to the damage as indicated by considerable difference in measured undamaged and damaged frequencies is analyzed using continuous wavelet transform. The position of the crack is located by sudden change in the spatial variation of the transformed response. This damage detection technique serves the purpose of structural health monitoring.

6.1. The experimental panel and data capture

The first stage of the work was to fabricate the stiffened panel (Figure 19) of size (adopted from reference K. Worden et al. (2003) 750x500x3mm, by the addition of two ribs composed of lengths of C-channel riveted to the short edges. Two stiffening stringers composed of angle section with section width of 25 mm run along the length of the sheet. Damage was simulated by the introduction of a saw cut depth 'd' in the stringer at 250mm from the edge of the panel. For different values of $d = 6\text{mm}$ and 12mm investigation was carried out. The forced vibration tests were conducted with free-free boundary conditions for the panel, which was suspended using springs and nylon line. The length of the panel was equally divided into eight elements and width was divided into six elements to give 8x6 meshes. For the undamaged and damaged panel frequency response functions were acquired. As shown in Figure (19) AB is along the line of the damaged stringer.

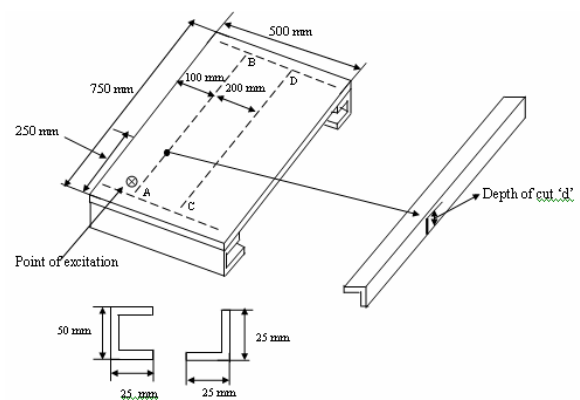


Figure 19. Details of the test panel

The system was excited at a distance of 107mm from the edge of the panel using an Electro dynamic shaker with force link driven by broad band white noise and response was picked up by piezo electric accelerometer and sampled by a Data Acquisition System (Dac-tron). FRF's were acquired at each point of

the mesh i.e. 48 points with exciter location fixed. The frequency range over which Frequency Response Functions between the accelerometer and exciting force were taken was 0-300 Hz.

The FRF's for the typical location before and after damages are plotted as shown in Figure 20. It shows a clear shift in frequencies. Also observed that zoomed view of in the frequency range from 100 to 150 Hz corresponding to the sixth mode (bold letters in Table 4). This shows that orders decrease in frequencies with respect to increase in damage. The acquired FRF's at 48 different locations were input to the LMS CADA PC MODAL software to get the experimental natural frequencies and mode shapes.

The mode shape data corresponding to sixth mode was analyzed using wavelet transform. Because of sparse sampling the wavelet transform if implemented directly would detect many points of sampled data as damage. Therefore to smooth the transition from one point to another over, sampling procedure was

necessary for that purpose a two dimensional cubic spline interpolation resulting in finer mesh of 15x21 points.

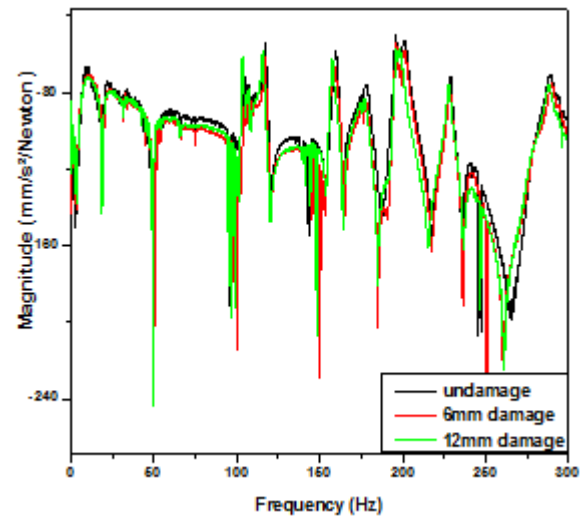
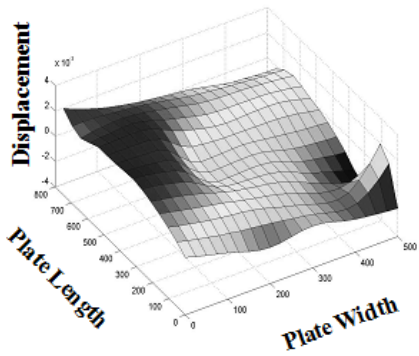


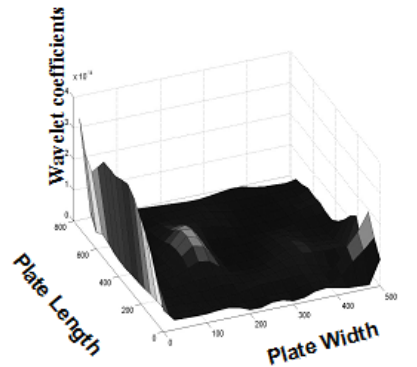
Figure 20. FRF's for undamaged and damaged panel

Table 4. Comparison of natural frequencies (Hz) for undamaged and damaged cases

Panel details	Frequencies (Hz) for the Mode number						
	1	2	3	4	5	6	7
Undamaged	19.61	33.62	62.58	65.09	104.66	117.27	159.05
6mm damage	19.72	33.52	63.16	65.58	104.65	117.05	153.16
12mm damage	18.74	33.32	62.60	65.24	104.40	115.64	156.76

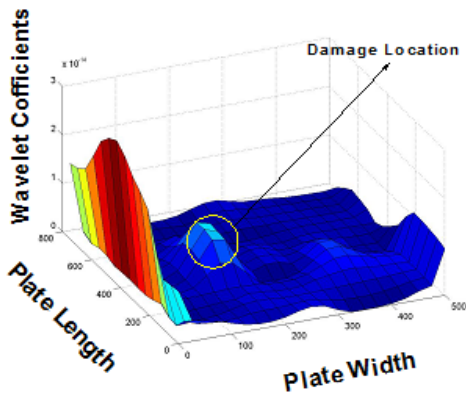


(21a)

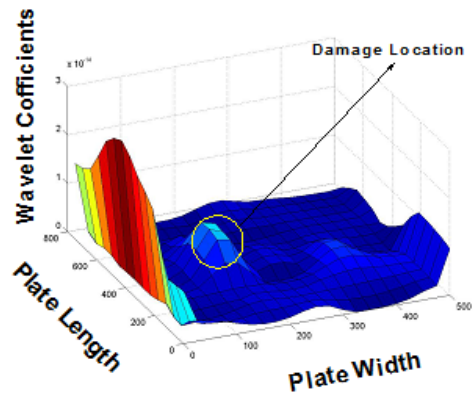


(21b)

Figure 21. (a) Mode shape of the undamaged panel, (b) Three-dimensional plot of wavelet coefficients for undamaged case at scale 0.01

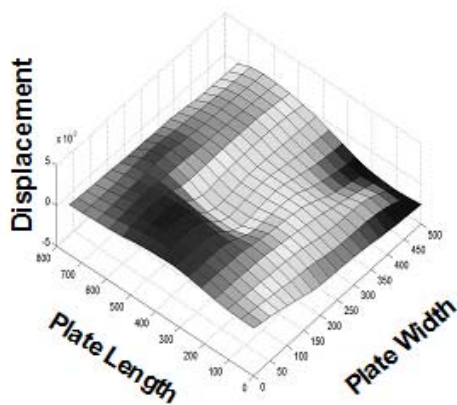


(22a)

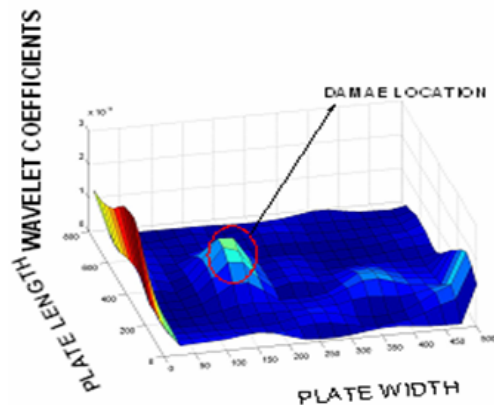


(22b)

Figure 22. (a) Mode shape of panel with damage level 6mm, (b) Three dimensional plot of Wavelet coefficients at scale 0.01



(23a)



(23b)

Figure 23. (a) Mode shape of the panel with damage level 12mm, (b) Three dimensional plot of wavelet coefficients at scale parameter $s = 0.01$

In order to detect the damage position, the mode shape was wavelet transformed using complex Gaussian wavelet with four vanishing moment with scale 0.01. Figure 21a and 21b shows the undamaged mode shape of (sixth mode) plot, three dimensional wavelet coefficients plot respectively.

Similarly Figure 22a and 22b and Figure 23a and 23b, show similar plot for 6mm and 12mm case of damage. It can be seen that there is a small peak region of high wavelet coefficients with bright area which indicates the existence of damage. Comparing Figure 22(b) and Figure 23(b) it can be concluded that as the damage level increases for 6mm to 12mm the maximum value of wavelet coefficients also increases at the damage location

6. Conclusions

The objective of this paper is to apply spatial wavelet transform to highlight the sensitivity for detection and localization of damage in a plate structure with all boundaries fixed, using mode shape and strain energy data as input. It is observed that by using modal data as input, damage can be identified exactly if the reduction in thickness is more than 10%. Below 10% reduction in thickness strain energy data input to wavelet is more sensitive.

Lipschitz (Hoelder) exponent (α) and Intensity factor (K) is derived from the coefficients to quantify the relation between damage and change in wavelet coefficients derived from modal and elemental strain energy data.

The variation of maximum absolute wavelet coefficients versus percentage of damage for different mode shapes and scales are studied. For damages near the boundaries with all edges free as boundary conditions the identification of damage is very difficult due to high wavelet coefficients near boundaries. In such cases the sensitivity of identifying damage can be increased by plotting the wavelet coefficients in logarithmic scale instead of using linear scale, where as in fixed boundary condition the method is able to identify dam-

age directly with out the need to plot coefficients in logarithmic scale.

In order to test the feasibility of applying proposed wavelet based damage identification method to experimental data (mode shape), experimental modal analysis is carried out on a simple steel beam and a stiffened panel with free-free boundary condition. This is particularly necessary because the experimentally obtained mode shape is distorted with noise. Hence the effectiveness of the method with noisy mode shape as input can be investigated. Three dimensional plots were clearly able to locate damage by increase in amplitude coefficients at the damage location for damage level. By plots conclude that this wavelet based damage identification method strongly depends on the measurement methods used to acquire spatial data, the accuracy and the measurement noise. This method is particularly suitable, when the vibration data is obtained from laser vibrometer or optic fiber sensor (non-contact type) which provides data with high accuracy and high spatial density.

References

- [1] Liew, K. W. and Wang, Q. 1998. Application of wavelet theory for crack Identification in structures. *Journal of Engineering Mechanics*, 124: 152-157.
- [2] Wang, Q. and Deng. X. 1999. Damage detection with spatial wavelets. *International Journal of Solids and Structures*, 36: 3443-3468.
- [3] Quek, S., Wang, Q. Zhang, L., and Ang, K. 2001. Sensitivity analysis of crack detection in beams by wavelet techniques. *International Journal of Mechanical Sciences*,. 43: 2899-2910.
- [4] Abdo, M. A. B. and Hori, M. 2001. A numerical study of structural damage detection using changes in the rotation of mode shapes. *Journal of sound and vibration*, 251, 2: 227-239.
- [5] Hong, J. C., Kim, Y. Y., Lee, H.C., and Lee, Y. W., 2002. Damage detection us-

- ing Lipschitz exponent estimated by the wavelet transform: applications to vibration modes of a beam. *International Journal of Solids and Structures*. 139, 1803-1816.
- [6] Kim, T. J., Ryu, Y. S., Cho, H. M., and Stubbs, N. 2003. Damage identification in beam type structures: frequency based method vs. mode shape based method, *Engineering Structures*, 1, 25: 57-67.
- [7] Douka. E., Loutridis. S and Trochidis. A. 2004. Crack identification in plates using wavelet analysis. *Journal of sound and vibration*. 270: 279-295.
- [8] Chang, C. C. and Chen, L. W. 2004. Damage detection of a rectangular plate by spatial wavelet approach, *Journal of Applied Acoustics*. 65: 819-832.
- [9] Chang, C. C. and Chen, L. W. 2005. Detection of the location and size of cracks in the multiple cracked beam by spatial wavelet based approach. *International Journal of mechanical systems and signal processing*, 19: 139-145.
- [10] Rucka. M. and Wilde. K, 2006, Applications of continuous wavelet transform in vibration based damage detection method for beam and plates. *Journal of sound and vibration*, 15: 143-149.
- [11] Grossmann, A. and Morlet. J. 1984. Decomposition of hardy functions into square integrable wavelet of constant shape. *SIAM Journal of Mathematical Analysis*, 15: 723-736.
- [12] Mallat, M. 1989. A Theory for Multi-resolution Signal Decomposition: The Wavelet Representation. *IEEE, Pattern Analysis and Machine Intelligence*, 11, 7: 659-674.
- [13] Daubechies 1992. Ten Lectures on Wavelets. Presented in *CBS-NSF Regional Conference in Applied Mathematics*.